Electronic Supplementary Information for

Sources of activity loss in the fuel cell enzyme bilirubin oxidase

Kulveer Singh, Trevor McArdle, Patricia R. Sullivan and Christopher F. Blanford

Table of contents

Section S1 Material sources

Bilirubin oxidase from *Myrothecium verrucaria* (*Mv*BOx) was obtained from Amano Enzyme. The enzyme was purified as for protein crystallization.[1] Lyophilized *Mv*BOx powder was dissolved in 10 mM sodium phosphate, pH 7.0 at 4 °C, then centrifugally dialyzed to remove small-molecular-weight contaminants (Vivaspin, 30 kDa MWCO PES). This was then further purified by weak anion exchange (DEAE Sepharose) and by hydrophobic interaction (HiTrap Phenyl Sepharose) chromatography at 4 °C. The protein was eluted using 10 mM sodium phosphate, pH 7.0 at 4 °C, with a 0–0.4 M ammonium sulfate gradient for the anion exchange, and 50 mM sodium phosphate, pH 6 at 4°C, with a 1.25–0 M ammonium sulfate reverse gradient for hydrophobic interaction. Typical yields of purified protein were ≈ 3% by mass. Protein concentrations were determined using the Beer-Lambert law based on A_{280nm} measured from enzyme aliquots and using $\varepsilon_{280nm} = 9.52 \times 10^4$ M^{-1} cm^{-1}, calculated from the enzyme amino acid sequence by the online software ProtParam – Expasy Proteomics Server (http://www.expasy.ch/tools/protparam.html).

Laccase from *Trametes versicolor* (TvL) was obtained as a crude powder from Sigma. The crude powder was dissolved in 10 mM sodium acetate, pH 5.5 at 5 °C, then filtered through two filters (GFA, 0.45 μm, 0.22 μm). This was then centrifugally dialyzed to remove small-molecular-weight contaminants (Vivaspin, 30 kDa MWCO PES). This was then further purified by weak anion exchange (Q Sepharose, 10 mM sodium acetate, pH 5.5 at 5 °C, with a 0–0.1 M ammonium sulfate gradient) followed by hydrophobic interaction (HiTrap Phenyl Sepharose, 20 mM sodium phosphate, pH 4.7 at 5 °C, with a 1.65–0 M ammonium sulfate reverse gradient) at 5 °C.

Dimethyl sulfoxide (DMSO, ≥99.9%, Fisher), hydroxylamine hydrochloride (>97%, Fisher), hydrochloric acid (37%, Fisher), sodium dihydrogen orthophosphate dihydrate (99.0–101.0%, Fisher), disodium hydrogen orthophosphate anhydrous (99.5+%, Fisher), trisodium citrate dihydrate (≥99%, Sigma), citric acid monohydrate (≥99%, Sigma), ammonium bicarbonate (≥99.5%, Sigma), iodoacetamide (≥99%, Sigma), dithiothreitol (DTT, ≥99.5%, Sigma), trypsin (from porcine pancreas, >10,000 units/mg, Sigma), pepsin (from porcine gastric mucosa, ≥250 units/mg, Sigma), tris(2–carboxyethyl)phosphine hydrochloride (TCEP, >98%, Sigma), sulphuric acid (1.83 g ml^{-1} specific gravity, >95%, Fisher), hydrogen peroxide (30% w/v, Scientific Laboratory Supplies), 3-mercaptopropionic acid (3MPA, >99%, Fluka), 3-mercapto-1-propanol (3MPOL, 95%, Sigma), 3,3´-dithiobis(sulfosuccinimidylpropionate) (DTSSP, >98%, ProChem Inc.). The *N*-hydroxysuccinimide ester of fluorescein-5-EX (F5EX, CAS no. 1196157-68-2) was purchased from Sigma Aldrich, stored in the dark at –20 °C. All chemicals were used as received without further purification. All

water was purified via reverse osmosis and ion exchange to a resistivity of 18.2 MΩ cm at 25 °C using a MilliQ water purifier.

Section S2 Equipment

QCM-D data were acquired using a Q-Sense E1 system with accompanying Q-Soft data acquisition software. QCM-D measurements without concurrent electrochemical analysis used a Q-Sense Flow module 401 (total volume ~140 µl, volume above sensor surface ~40 µl, non-sensor surfaces Ti or Viton). E-QCM-D measurements used a modified Q-Sense QEM401 module (volume above sensor surface ~100 µl). The PTFE insert on the electrochemistry module was replaced by a custom-made insert made of poly(oxomethylene) (Delrin) for better wettability, to accommodate a standard 5.7 mm OD reference electrode, and to provide a more robust seal when liquid was pulled through the cell. The manufacturer's value for typical mass sensitivity in liquid is 1.8 ng cm^{-2},[2] equivalent to <0.3% of a monolayer of *Mv*BOx.

The sensors (Q-Sense) were 14mm diameter, gold-coated, AT-cut quartz crystals with a Ti adhesion layer and a fundamental frequency of (4.95 ± 0.05) MHz. All the frequency and dissipation changes presented are from the seventh harmonic of the fundamental frequency (35 MHz, C = 125 ng cm^{-2} Hz^{-1}). This harmonic is less affected by crystal mounting and small mechanical vibrations when changing solutions, is more surface sensitive, and still gives a good signal-to-noise ratio compared to the higher frequencies. The measured temperature of the QCM cell was constant within 10 mK. The dependence of the fundamental frequency on temperature (i.e., d($\Delta f/f$)/dT) of AT-crystals at 25 °C is -3.3×10^{-7} K^{-1},[3] so temperature variations should not lead to frequency variations greater than 16 mHz. In practice, however, we observed larger variations in frequency and dissipation, usually in the range of ±7–14 Hz and ±0.5 ppm for Δf_7 and Δd_7, respectively. The sensor surface is remote from the point at which the E1 system measures the temperature, so the entire liquid handling system (cell, reservoir, tubing and pump) was placed on top of an aluminium plate through which water held at 25 °C was circulated, then surrounded by an insulated box in which the air was circulated by an electric fan. The thermal coupling between the flow modules and QCP101 chamber platform was improved with thermal conducting paste (RS components, RS 217-3835). Other sources of variation arise from the mounting of the crystal in the cell and the effect of the repeated cleaning procedure on the gold surface.

Enzyme was introduced to the cell by stopping the pump, reversing the flow for a few seconds to produce a suspended drop at the end of the entry tube, placing the tube in the enzyme solution and restarting the pump in the forward direction. After enzyme was introduced, the procedure was repeated to flow buffer through the cell. Each exchange took less than 1 min. The dead time for liquids to flow from the inlet to the cell was 2 min.

The electrochemical cell used a three-electrode configuration: the gold-coated QCM sensor (exposed geometric area of 0.80 cm^2) as the working electrode; a 0.2mm thick, 2.25cm^2 square platinum plate running parallel to the sensor surface as the counter electrode; and a Ag|AgCl|3M NaCl reference electrode (BASi RE-6, $E_{SHE} = E_{ref} + 0.209$ V). The distance between the working electrode and counter electrode was 0.7–0.8 mm; the distance between working and reference electrode was 0.9–1.0 mm. The potential was set and the current was measured by an Ivium CompactStat, using the accompanying IviumSoft control software.

Buffer was kept in a sealed glass bottle and oxygenated for 20 min before each experiment. Increasing the pump speed produced moderate increases in current. For example, an O_2-reduction current of –69 µA at 0.1 ml min^{-1} increased by 9% when the flow rate was increased to 0.3 ml min^{-1}. No significant current increase was seen upon increasing the flow rate to 0.5 ml min^{-1} and flow rates greater than 0.5 ml min^{-1} mechanically disrupted the stability of the electrochemical cell. (Conditions for example: 25 µl of 12 mg ml^{-1} *Mv*BOx, 25 °C, 0.1 M sodium phosphate pH 6.0, 0 V vs. reference.)

Section S3 QCM sensor surface treatment and protein adsorption

Section S3.1 Cleaning

Residual contamination on new QCM sensors was removed by placing them under a ozone-generating UV lamp in air for 30 min. Sensors were reused by oxidizing the surface with piranha solution (3:1 v:v conc. H_2SO_4:30 wt% H_2O_2) for 20 min with constant heating at 60°C, followed by rinsing in water. The crystals were dried under a stream of house nitrogen from boil-off, then ozone treated as described.

Section S3.2 Organothiol surface modification

Surface modification solutions consisted of either 10 mM DTSSP, 10 mM 3MPA or 10 mM 3MPOL mixed with 1.3 mM TCEP in ethanol. Solutions were sonicated for 20 min. before freshly cleaned sensors were immersed for 15 h under a nitrogen atmosphere (for 3MPA) or 3 h in air (for DTSSP). (Consistent with the reports of Z. Cao and co-workers, we have observed gold dissolution by QCM from oxygenated thiol solutions.)[4, 5] Surface coverage of the thiol layer was determined by reductive desorption in basic anaerobic aqueous solution,[6] giving surface coverages between 9.6 $x10^{-11}$ and 6.7 $x10^{-10}$ mol cm^{-2}, depending on the size and length of the thiol layer. After surface modification, the crystals are rinsed with water and ethanol, dried in a stream of nitrogen gas, then mounted in the E-QCM cell.

Section S3.3 Introduction of protein to the cell

The fluid flow through the cell is controlled via peristaltic pump located and operated outside the cell, at a rate of 0.1 ml min^{-1}. The pump was stopped and the inlet tubing switched to a microcentrifuge tube containing 25µL of protein at the desired concentration. After addition, the pump was temporarily switched

to flow in an anticlockwise to eliminate air bubbles from the flow path. At this point the pump was turned back to clockwise and the fluid flow was resumed.

Section S3.4 DTSSP coupling

The addition of protein was done in the same way however upon the QCM-D response in the frequency and dissipation traces, the peristaltic pump was turned off for 45 min to allow for the succinimidyl groups to react with the lysine residues of *Mv*BOx. After the reaction had proceeded the pump was turned back on and fluid flow resumed.

Section S4 Relating electrocatalytic current to enzyme activity

Electrocatalytic activity is related to the areal density of the enzyme on the surface and its turnover frequency according to Eqn. S1:

$$i = -n\,F\,A\,\Gamma\,k_{\mathrm{cat}} \tag{S1}$$

where i is the catalytic current (negative for reductive processes by convention), n is the number of electrons involved in the reaction (4 for the reduction of O_2 to $2H_2O$), F is Faraday's constant, A is the electroactive surface area of the electrode accounting for surface roughness (0.80 cm^2 × 1.6, see Section S7), Γ is the coverage of the enzyme (4.2 pmol cm^{-2} for a saturated monolayer, see Section S8), and k_{cat} is the enzyme's intrinsic rate constant/turnover frequency.

Section S5 Degree of labelling and reactive lysine determination

Section S5.1 Methods

Section S5.1.1 Fluorescein 5-EX (F5EX) labelling

*Mv*BOx was labelled with an amine-reactive fluorophore based on a procedure from Molecular Probes (now Invitrogen).[7] Aliquots of 15.2 mM F5EX in DMSO were mixed with aliquots of 0.24–0.25 mM *Mv*BOx in 0.1 M sodium bicarbonate pH 8.3 to give dye:protein molar ratios of up to 72. The total volume of the reaction mixture was 110 to 200 µl. The mixture was incubated in the dark with stirring at room temperature for 1 h, then 0.1 ml of freshly prepared 1.5 M hydroxylamine pH 8.5 was added to conjugate to unreacted F5EX and stop further reaction with the protein. The protein was separated from unconjugated dye by dialysis through a 30 kDa MWCO filter (Vivaspin, GE Healthcare).

The degree of labelling (DoL) was determined spectrophotometrically ($\lambda_{\mathrm{max}}^{\mathrm{F5EX}}$ = 494 nm) in a 1cm path length quartz cuvette and Eqn. S2:

$$\mathrm{DoL} = \frac{A_{494\ \mathrm{nm}}^{\mathrm{mix}}\ \varepsilon_{280\ \mathrm{nm}}^{\mathit{Mv}\mathrm{BOx}}}{\left(A_{280\ \mathrm{nm}}^{\mathrm{mix}} - \mathrm{CF}\ A_{494\ \mathrm{nm}}^{\mathrm{mix}}\right)\varepsilon_{494\ \mathrm{nm}}^{\mathrm{F5EX}}} \tag{S2}$$

where $A^{\text{mix}}_{280\text{ nm}}$ and $A^{\text{mix}}_{494\text{ nm}}$ are the recorded optical densities for the labelled protein at 280 nm and 494 nm, respectively, $\varepsilon^{\text{F5EX}}_{494\text{ nm}} = 6.8 \times 10^4\ \text{M}^{-1}\ \text{cm}^{-1}$, $\varepsilon^{\text{protein}}_{280\text{ nm}} = 9.2 \times 10^4\ \text{M}^{-1}\ \text{cm}^{-1}$, and the correction factor (CF) = 0.30. The correction factor is the ratio of the absorbance of the free dye at 280 nm to its absorbance at λ_{max} (i.e., $\varepsilon^{\text{F5EX}}_{280\text{ nm}}/\varepsilon^{\text{F5EX}}_{494\text{ nm}}$). The values for the dye were recorded at pH 8.0.

Section S5.1.2 Trypsin digest

Solutions of 1 mg ml^{-1} *Mv*BOx, 100mM dithiothreitol (DTT, for reduction of disulphide bonds in the protein), 100mM iodoacetamide (to cap free cysteine thiolates), and 20 µg ml^{-1} trypsin were made in 50mM ammonium bicarbonate. 2.1 µl of the DTT solution was added to 50 µl of the protein solution, the mixture was vortexed then incubated for 45 min at 37 °C. After the solution returned to room temperature, 8.7 µl of the iodoacetamide solution was added, the mixture vortexed again, then incubated in the dark for 45 min. at room temperature. A further 2.2 µl of DTT solution was added, the mixture vortexed, then incubated at 37 °C for 10 min. 20 µl of trypsin solution was added to the mixture, which was then incubated for 12 h at 37 °C. Final solution frozen at –21 °C and stored for 7 d until mass spec analysis.

Section S5.1.3 Pepsin digest

50 µl *Mv*BOx (15 mg ml^{-1}, 0.1M sodium phosphate buffer pH 6.0) was acidified with 20 µl 0.04M HCl. To this solution, 20 µl 0.3 mg ml^{-1} pepsin in water was added (71:1) and the mixture vortexed briefly. The mixture was incubated for 12 h at 37 °C, heated to 95 °C for 15 min. then cooled to room temperature and frozen at –21°C.

Section S5.1.4 MALDI mass spectrometry

All MALDI mass spectrometry experiments were carried out on an Ultraflex II instrument (Bruker Daltonics) in positive reflectron mode. A solution of matrix (α-cyano-4-hydroxycinnamic acid) matrix was applied to the protein sample and allowed to dry before analysis.

The spectra taken of the protein after the trypsin digest are plotted in Figure S1. Peaks were labelled according to the conventions of Roepstorff and Fohlman[8] and Johnson and co-workers,[9, 10] guided by the tutorial article from Wysocki and co-workers.[11] These assignments are summarized in Table S1 and Table S2. No differences were observed in the peak positions after the pepsin digest.

Section S5.2 Results and Analysis

At a dye-to-protein molar ratio of ca. 25, the degree of labelling saturated at about one dye molecule per protein molecule (DoL = 1.09 ± 0.10, Figure S1 inset). The main new contributions to the mass spectrum of the labelled protein were the peaks shown in Figure S1**B**, which correspond to Lys408 and Lys118. Small peaks appeared in fragments containing labelled Lys181 (Figure S1**E**) and Lys21 or Lys214 (Figure S1**F**). Small peaks disappeared from the spectrum of the unlabelled protein corresponding to Lys429 (Figure S1**D**)

and Lys44 (Figure S1**E&G**). Trypsin cleaves at Arg and Lys residues, so the F5EX labels will always be at the C-terminus of any peptide fragment. So, with the exception of the doubly charged a21 fragment in Figure S1**F**, a, b and c ions are not labelled. There was no definitive pair of labelled peaks corresponding to the appearance of one shifted by 475.07 Da and the disappearance of its parent.

Most of the lysines can be ruled out: of the 11 lysines in the sequence of *Mv*BOx (Figure S2), three do not appear differently in the labelled and unlabelled samples: Lys220, Lys251 and Lys314. Lys118 and Lys429 have <2.5 $Å^2$ of their atoms on the protein surface (using the FindSurfaceResidues.py algorithm on PyMOLwiki).[12] Although Lys118 is accessible to react with dye molecules, it is too buried to couple to surface groups.

The strongest evidence points to the most reactive exposed lysine side chain being Lys408, with some reactivity in Lys 21 and Lys181. All three groups are more than 1.5 nm from the enzyme's active sites, too far for tunnelling rates compatible with biological processes:[13] Lys408 is 2.59 nm from the type 1 copper (considered the primary electron acceptor)[14] and 2.15 nm from the type 2 copper; Lys21 is 3.23 nm from the type 1 and 2.03 from a type 3 copper; and Lys181 is 1.94 nm from the type 1 copper. These distances were measured from the terminal nitrogen atom.

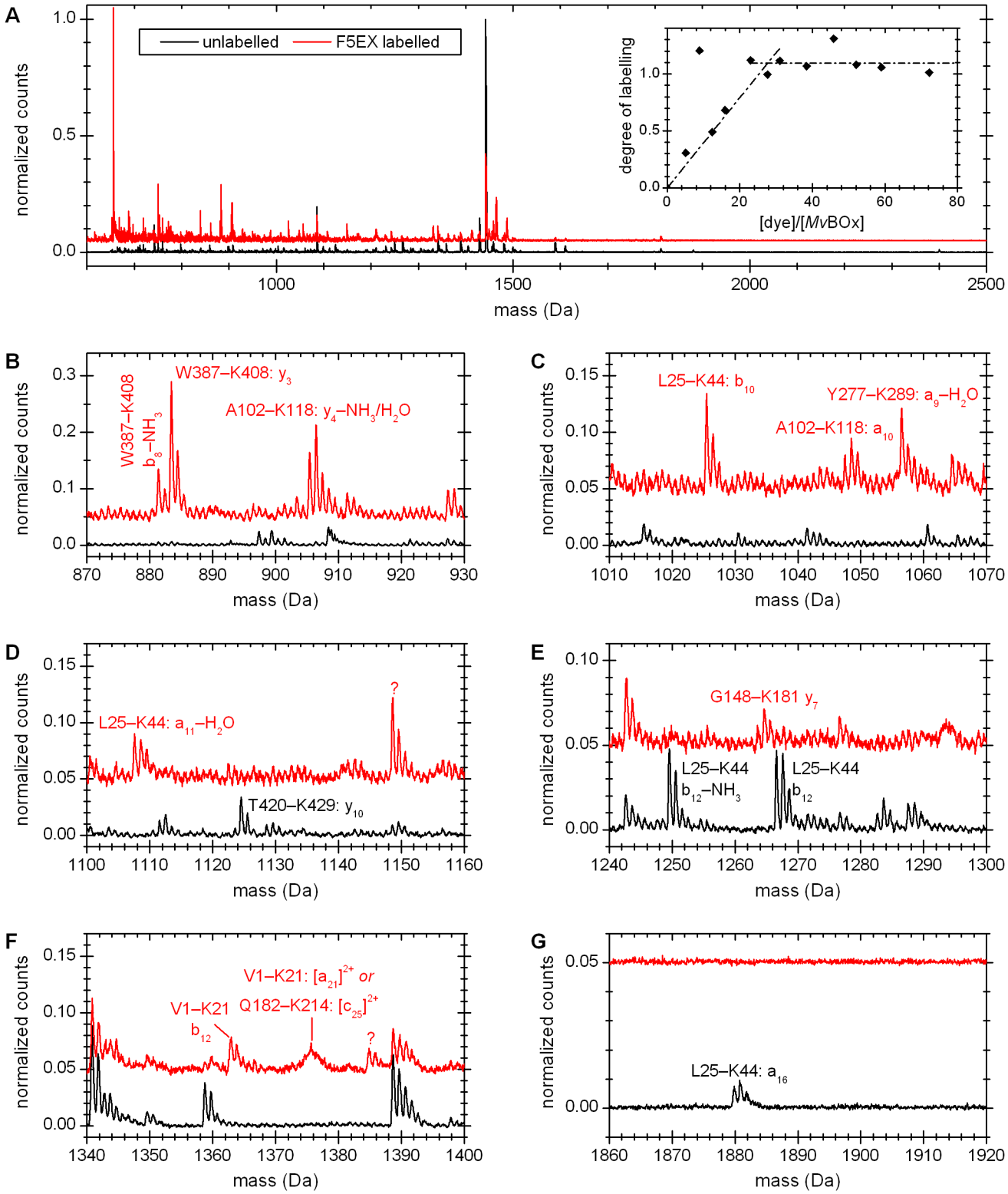

Figure S1. Determination of the location of reactive lysine side chains in *Mv*BOx by reaction with fluorescein 5-EX (F5EX). Panel **A** compares the full MALDI mass spectra of enzyme that has been labelled with F5EX (red) and that which has not (black). The inset shows the degree of labelling as a function of enzyme concentration. The lines are to guide the eye. Panels **B**–**F** show specific regions where the two mass spectra differ. Peak labels give the peptide sequence and ion type.[8-10] The full scale for the unlabelled and labelled spectra are 2.9×10^4 and 1.9×10^4 counts, respectively.

Table S1. Additional peaks in MALDI mass spectrum of fluorescein 5-EX–labelled *Mv*BOx compared to unlabelled *Mv*BOx after trypsin digest

Mass (Da)	Fragment	Assignment
881.4	W387–K408	$b_8–NH_3$
884.4	W387–K408	y_3
905.4	A102–K118	$y_4–H_2O/NH_3$
1025.5	L25–K44	b_{10}
1048.5	A102–K118	a_{10}
1056.5	Y277–K289	$a_9–H_2O$
1107.6	L25–K44	$a_{11}–H_2O$
1148.5	unknown	
1264.6	G148–K181	y_7
1362.8	V1–K21	b_{12}
1374.	V1–K21 Q182–K214	a_{21}^{2+} c_{25}^{2+}
1384.9	unknown	

Table S2. Missing peaks in MALDI mass spectrum of fluorescein 5-EX–labelled *Mv*BOx compared to unlabelled *Mv*BOx after trypsin digest

Mass (Da)	Fragment	Assignment
1124.5	T420–K429	y_{10}
1249.5	L25–K44 Q182–K214	$b_{12}–NH_3$ c_{25}^{2+}
1266.6	L25–K44	b_{12}
1879.9	L25–K44	a_{16}

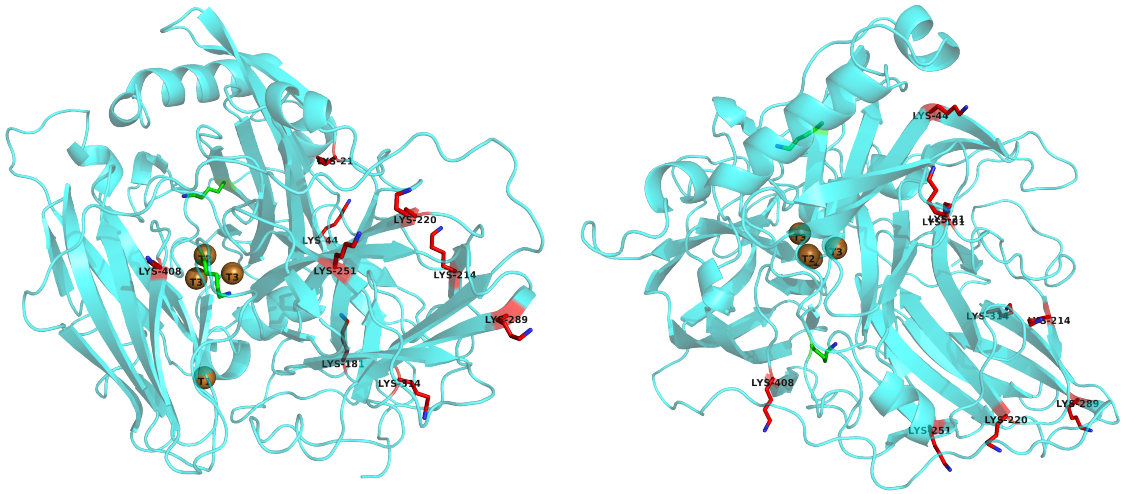

Figure S2. PyMOL visualization of the location of the lysine residues in *Mv*BOx (PDB code 2xll).[1] The polypeptide backbone is shown as the cyan cartoon. The coppers are shown as spheres labelled with their spectroscopic designation. The nine lysine side chains that have at least 2.5 $Å^2$ on the surface are in red; the two that do not are in green. The image on the right is rotated 90° along a horizontal axis.

Section S6 Effect of protein concentration on protein adsorption isotherm

Oxygenated buffer was flowed over gold-coated crystals modified with 3-mercaptopropionic acid (Figure S3) and those with no surface modification (Figure S4) until a steady baseline was observed in the frequency and dissipation traces. For each concentration, 25 µL of enzyme was flowed through the cell. Both sets show a maximum frequency change for the seventh harmonic of 275–325 Hz (0.70–0.83 µg cm^{-2}, cf. Section S8) The dissipation traces are markedly different: the adlayer on bare gold initially has a much higher viscoelasticity (i.e., higher dissipation) then stiffens within 1–2 min. There is also a much sharper decrease in mass after adsorption on bare gold. These are both characteristics of substantial dehydration and denaturation of the protein.

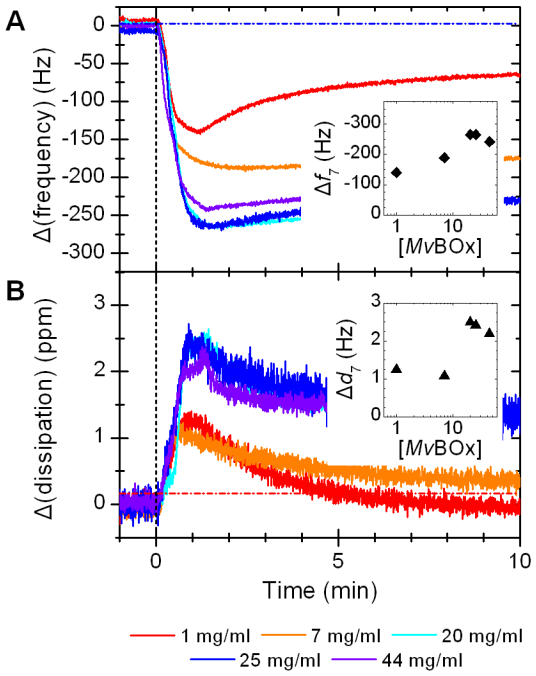

Figure S3. The effect of enzyme concentration on adsorption onto 3-mercaptopropionic acid–modified gold-coated quartz crystals. Panel **A** shows the frequency change at different concentrations of enzyme. Panel **B** shows dissipation change at different concentrations. The insets show the relationship between concentration and highest magnitude of frequency and dissipation change. Conditions: 7th harmonic, 0.1 M sodium phosphate pH 6.0 (pre-saturated with O_2), 25 °C, 0.1 ml min^{-1}

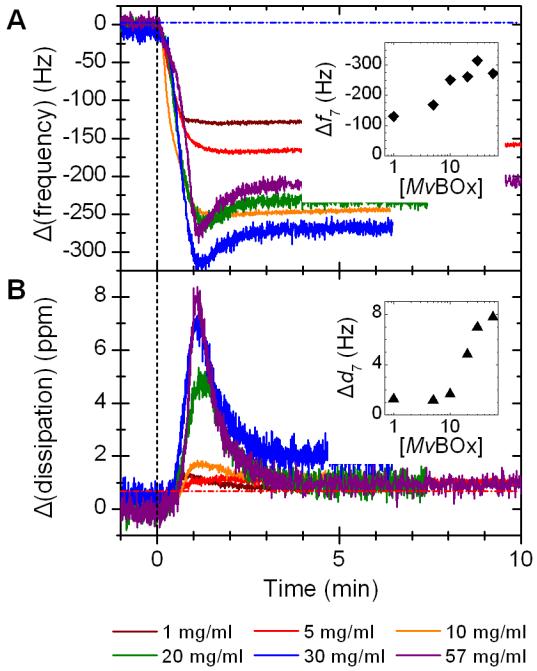

Figure S4. The effect of enzyme concentration on adsorption onto bare gold-coated quartz crystals (i.e., without organothiol modification). Panel **A** shows the frequency change at different concentrations of enzyme. The inset in panel **A** shows the relationship between concentration and peak frequency change. Panel **B** shows the dissipation change at different concentrations. The insets show the relationship between concentration and highest magnitude of frequency and dissipation change. Conditions: 0.1 M sodium phosphate pH 6.0 (pre-saturated with O_2), 25 °C, 0.1 ml min^{-1}

Section S7 Electroactive area (surface roughness) determination

The accessible surface area of the gold-coated QCM sensors was determined by the electrochemical formation and stripping of a gold oxide monolayer in solution according to an IUPAC method.[15] The QCM crystal was suspended in 0.1 M H_2SO_4, typically immersing 90 mm^2 of the gold surface. The potential was cycled at 50 mV s^{-1} from 0.45 V to 1.6 V (vs. Ag|AgCl|3 M NaCl) until a stable voltammogram was recorded (30 cycles). The potential was then cycled once over the same range at 10 mV s^{-1} and the charge transferred was calculated from the stripping peak at about 1.08 V vs. ref, corrected with a linear baseline (Figure S5). Backscattered electron images of the sensor surface (Figure S6) appeared to show a polycrystalline surface with a profusion of 5µm-wide cracks. We used the IUPAC-recommended value of 390 ± 10 µC cm^{-2} to relate the area of the stripping peak to the surface area of the gold accessible to oxygen.[15] The ratio of the electrochemically accessible surface area to the geometric surface area (roughness factor) was 1.5–1.6. These roughness factors are consistent to those reported by Kamitaka et al. for their Seiko sensors (1.5–1.7).[16]

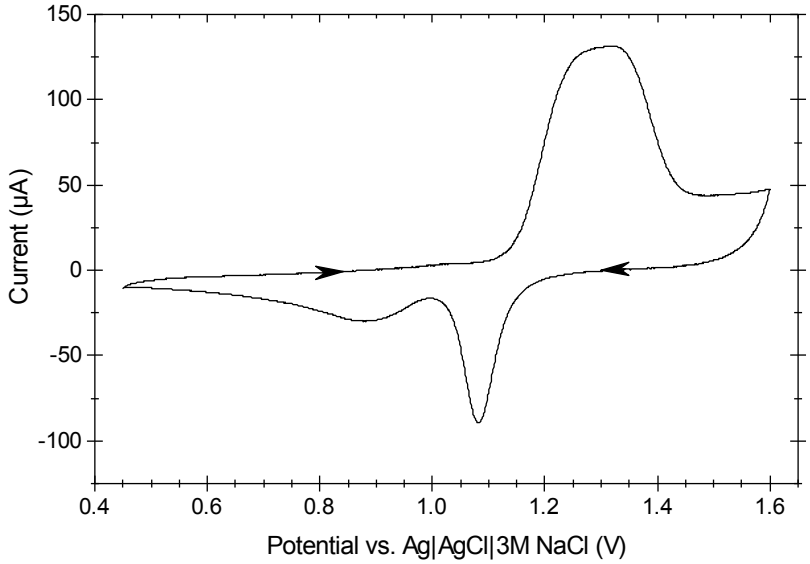

Figure S5. A representative example of the final cyclic voltammogram associated with gold oxide formation and stripping on a Q-Sense QCM sensor.

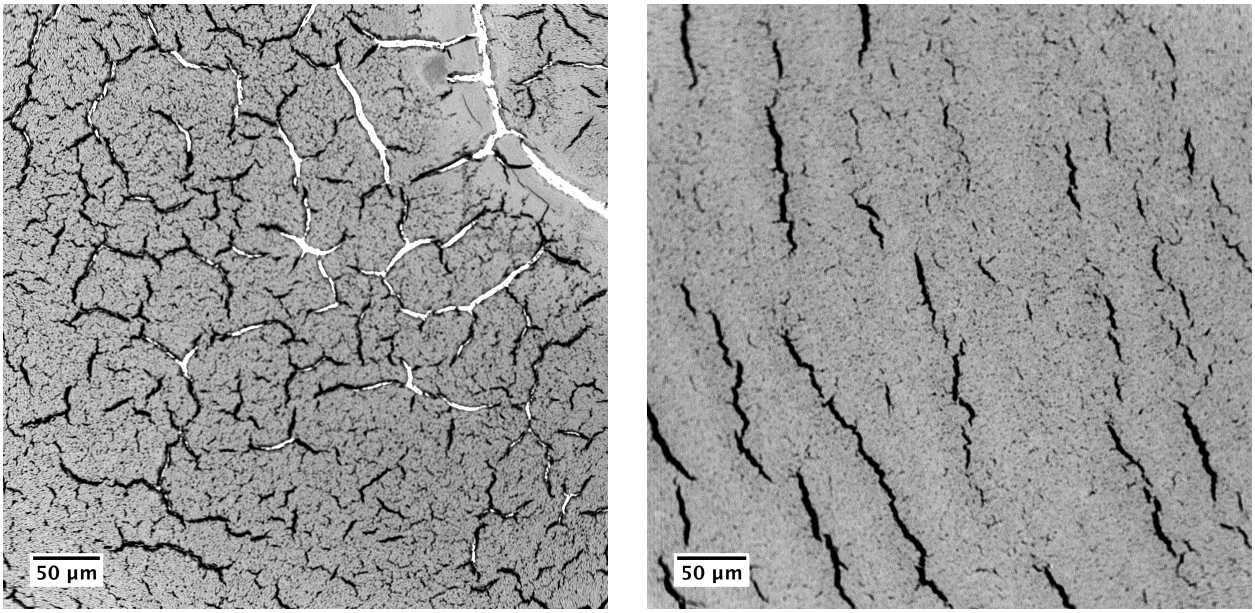

Figure S6. Representative scanning electron micrographs taken of the surface of a Q-Sense gold-coated QCM sensor. The image on the left was taken near the crystal centre and the right image was taken toward the edge of the crystal. The crystals were new and were prepared by leaving under an ozone-generating lamp for 20 min. The above images are from a backscattered electron SEM (Phenom Pro G2 desktop SEM).

Section S8 Estimation of the mass required for surface saturation

A first estimate of the frequency change expected from a saturated monolayer of *Mv*BOx can be obtained by simply dividing the QCM sensor's active area by the macromolecule's footprint (ca. 40 nm^2, based on PDB 2xll),[1] then applying the Sauerbrey equation:[3]

$$\Delta m = -\frac{\sqrt{\rho_q \mu_q}}{2 f_1^2 N} \Delta f_N \tag{S3}$$

$$\Delta m = -\frac{C}{N} \Delta f_N \tag{S4}$$

where Δm is the mass adsorbed, ρ_q and μ_q are the density and shear modulus of AT-cut quartz (2.648 g cm^{-3} and 2.947×10^{11} g cm^{-1} s^{-2}, respectively), f_1 is the fundamental frequency of the sensor (4.95 ± 0.05 MHz), N is the harmonic of the sensor, and Δf_N is the frequency change of that harmonic. For the Q-Sense E1, the proportionality constant, C, is 17.87 ng cm^{-2} Hz^{-1}.

Table S3. Contributions to the hydrated mass of *Mv*BOx

Component	Mass (Da)
peptide chain	59955
copper ions four per macromolecule	254
ordered glycans four *N*-linked *N*-acetylglucosamines per macromolecule	812
water V_{cell} = 631.75 nm^3, 4 macromolecules/cell assumes 53.3% solvent, ρ_{water} = 10^{-21} g nm^{-3} (of which there are 316 ordered water molecules per macromolecule = 5922 Da)	50520
total	*111541*

Monolayer coverage of close-packed *Mv*BOx macromolecules on a perfectly smooth sensor surface is 4.2 pmol cm^{-2}. Corrections must be applied for the roughness of the sensor surface (Section S7) and the mass of the water that is mechanically coupled to the protein. We assumed that solvent content of the three-dimensional X-ray structure could approximate the mass of water in a closely packed monolayer of the protein to calculate a hydrated mass of 111.5 kDa (Table S3). This gives a maximum adsorbed mass on a smooth electrode of 0.47 µg cm^{-2} (Δf_1 = –26.0 Hz, Δf_7 = –182 Hz), and 0.78–0.80 µg cm^{-2} on our electrodes (Δf_1 = 44 Hz, Δf_7 = –306–308 Hz, 7.2 pmol cm^{-2}). The latter values are consistent with the observations presented in the main text.

Section S9 Enzyme adsorption on a bare gold sensor

The measurements shown in Figure S7 parallel those shown in Figure 1 in the main text. The change in frequency occurring here is to a lesser extent than with the 3MPA-modified gold surface and the magnitude of catalytic current is also lower, within the normal range of variation we observed. When a chronoamperometric potential is applied (~28 min) there is a large apparent mass loss (~25 Hz, 0.06 µg cm^{-2}) which may be due to removal of loosely bound enzyme or mechanical effects (cf. Figure 2 in the main text). The short, horizontal portion of the current vs. dissipation trace (Figure S7 inset) arose from a short increase in dissipation after the potential was turned on, after which the trace returned to its more typical linear correlation with a slope near 1. The first-order time constant for current loss was 2.2 h.

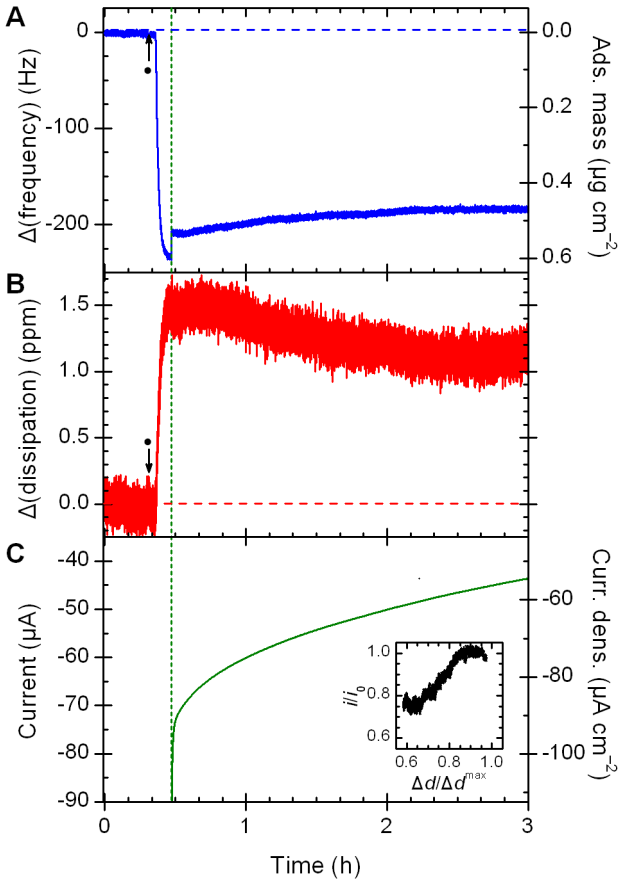

Figure S7. E-QCM-D response (7th harmonic) with time for bilirubin oxidase adsorbed on a bare gold crystal surface: **A** frequency change, **B** energy dissipation change, **C** O_2 reduction current. Circle (●) indicates when 25 µl 24 mg ml^{-1} *Mv*BOx was injected. Green dashed line shows when a potential of 0.21 V vs. SHE was applied. Inset in C shows the correlation between dissipation and electrocatalytic current. Conditions: 0.1 M sodium phosphate pH 6.0 (pre-saturated with O_2), 25 °C, 0.1 ml min^{-1}. Current density based on geometric area of 0.80 cm^2.

Section S10 Combined effects of cyclic voltammetry and chronoamperometry

We compared the effects of constant and variable potentials on the same layer of *Mv*BOx (Figure S8). After *Mv*BOx adsorption, the potential was cycled five times (Figure S8B, scan time 124 s) causing a 25% mass loss (ca. 0.15 µg cm^{-2}) and an activity loss of about a third (44 µA). The shape of the first reductive scan shows flattening that is characteristic of mass-transport limitations, which would mask the true activity of the protein layer, so the actual activity loss is probably higher. At 0.45 V, the activity loss is about 60%. The potential was then held constant at 0 V for ca. 7 h. During this time the frequency trace remained relatively stable between –146 and –132 Hz, but the current dropped by 52%. Turning the potential on and off caused momentary fluctuations in the frequency trace, similar to that seen in Figure S7. Finally, the potential was cycled 10 more times (Figure S8C) during which the activity dropped by about a third and the mass dropped by about a tenth to about 60% of its value before the start of the voltammetry.

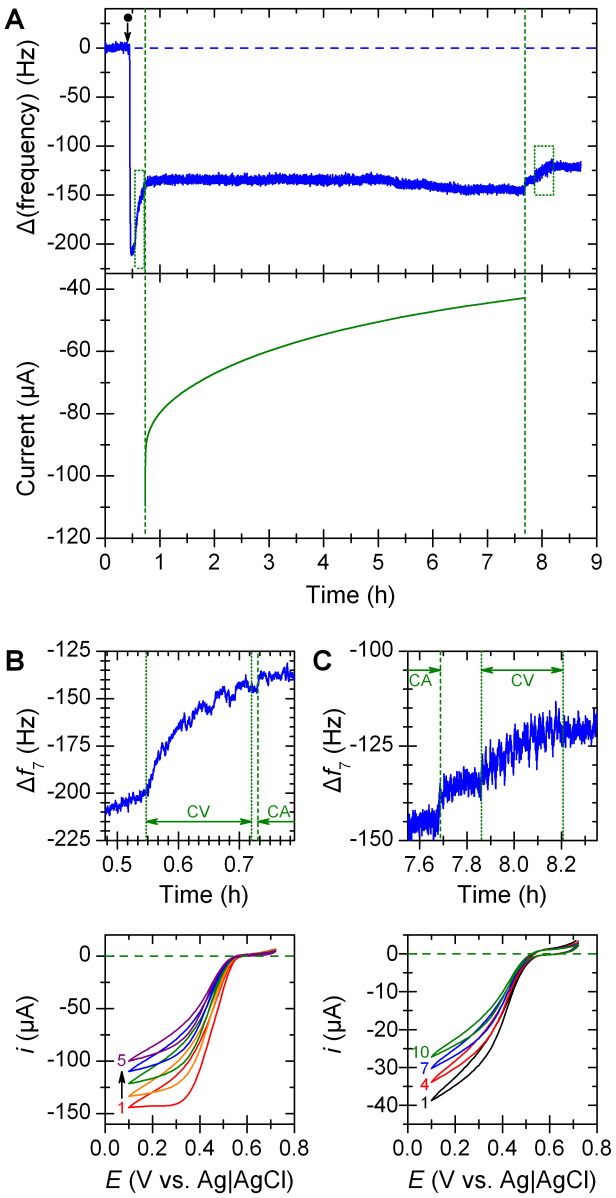

Figure S8. Frequency and current responses with time for *Mv*BOx adsorbed on a gold-coated QCM sensor modified with 3-mercaptopropionic acid. The top part of panel **A** shows the frequency change. Circle (●) indicates when 25 µl 24 mg ml^{-1} *Mv*BOx was injected. The periods when the potential was cycled (panels **B** and **C**) are indicated by dotted green boxes. The period when a constant reducing potential was applied is indicated by dashed green vertical lines. The bottom part of panel **A** shows current response to constant potential. Panel **B** shows frequency and current responses to five potential cycles before a constant potential was applied. Panel **C** shows this data for 10 potential cycles after a constant potential was applied. Data for frequency traces averaged over 21 points (6 s). Conditions: 0.1 M sodium phosphate pH 6.0 (pre-saturated with O_2), 25 °C, 0.1 ml min^{-1}, seventh harmonic shown. Cyclic voltammetry (CV): 0.72 → 0.10 → 0.72 V vs. Ag|AgCl|3M NaCl, 10 mV s^{-1}. Chronoamperometry (CA): constant applied potential of 0 V vs. Ag|AgCl|3M NaCl.

Section S11 QCM measurements in the absence of electrocatalysis

Cycling the potential on thiol-modified gold crystals without enzyme (Figure S9) produces oscillations in the Δf & Δd traces as for Figure 1, but with an amplitude about three times higher than when *Mv*BOx or BSA is adsorbed. The traces in panel C show the onset of O_2 reduction around 0.5 V vs. SHE. A bump on the oxidative scan appears around 0.72 V vs. SHE after the first scan.

Bovine serum albumin (BSA), a globular protein with similar dimensions to *Mv*BOx, was adsorbed on a 3MPA-coated QCM sensor (Figure S10). Unlike the rapid mass loss observed for an *Mv*BOx adlayer when the potential was cycled (Figure 2), the frequency response for the BSA adlayer increased slightly to a value about 80% of its initial magnitude. The frequency response of an azide-inhibited *Mv*BOx adlayer (Figure S11) was closer to that of the uninhibited enzyme, with a large, rapid drop in adsorbed mass. As expected, no electrocatalytic activity was observed for either BSA or azide-inhibited *Mv*BOx.

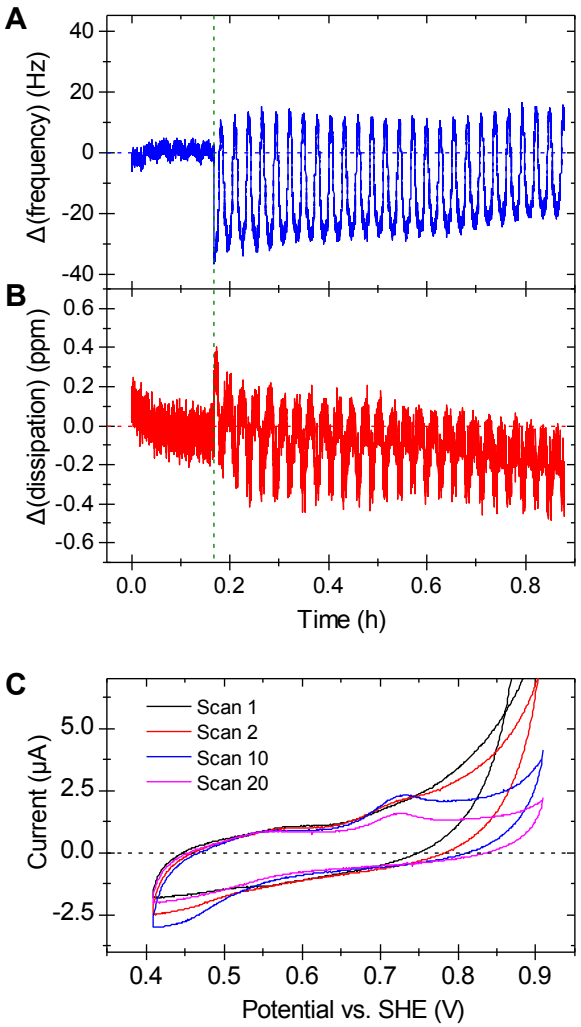

Figure S9. Frequency, dissipation and cyclic voltammetric responses with time for a gold-coated QCM sensor modified with 3-mercaptopropionic acid. Panel **A** shows the frequency change, panel **B** shows the dissipation response and panel **C** shows selected CV traces. The vertical green dashed line indicates the start of the voltammetry. Conditions: 0.1 M sodium phosphate pH 6.0 (pre-saturated with O_2), 25 °C, 0.1 ml min^{-1}, seventh harmonic shown. Cyclic voltammetry: 0.7 → 0.2 → 0.7 V vs. Ag|AgCl|3M NaCl, 10 mV s^{-1}.

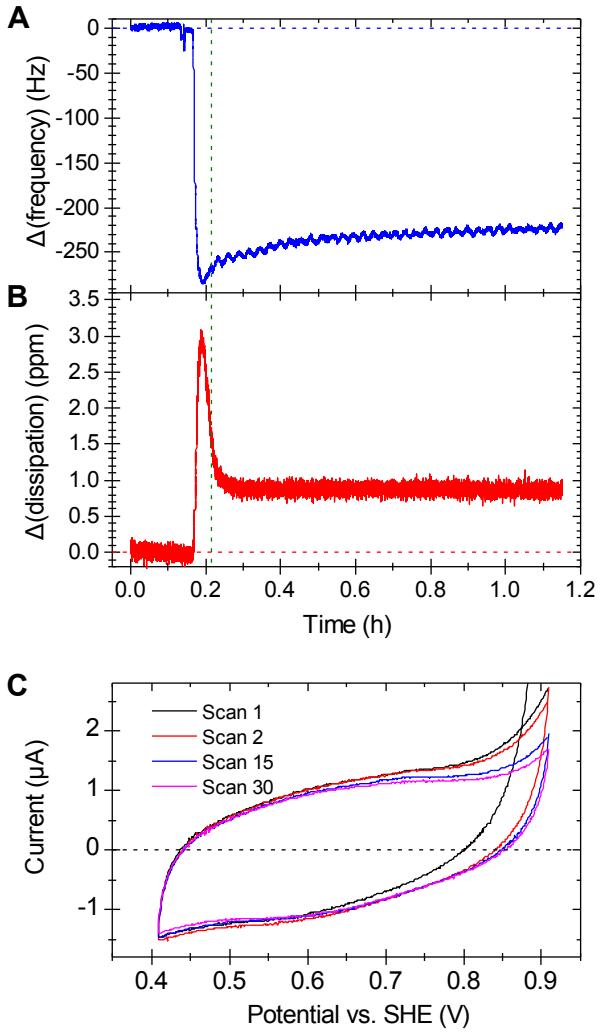

Figure S10. Frequency, dissipation and cyclic voltammetric responses with time for bovine serum albumin (25 µl 24 mg ml^{-1}) adsorbed on a gold-coated QCM sensor modified with 3-mercaptopropionic acid. Panel **A** shows the frequency change, Panel **B** shows the dissipation response, and Panel **C** shows selected CV scans. The vertical green dashed line indicates the start of the voltammetry. Conditions: 0.1 M sodium phosphate pH 6.0 (pre-saturated with O_2), 25 °C, 0.1 ml min^{-1}, seventh harmonic shown. Cyclic voltammetry: 0.70→ 0.20 → 0.70 V vs. Ag|AgCl|3M NaCl, 10 mV s^{-1}.

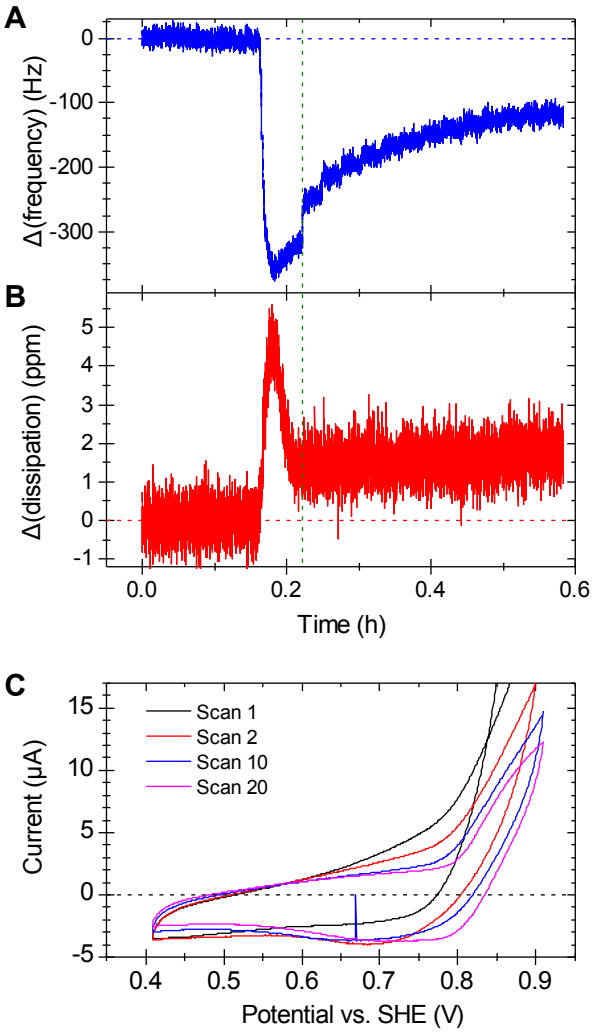

Figure S11. Frequency and current responses with time for *Mv*BOx inhibited with 0.1 mM azide (25 µl 24 mg ml^{-1}) adsorbed on a gold-coated QCM sensor modified with 3-mercaptopropionic acid. Panel **A** shows the frequency change, Panel **B** shows the dissipation response, and Panel **C** shows selected CV scans. The vertical green dashed line indicates the start of the voltammetry. Conditions: 0.1 M sodium phosphate pH 6.0 (pre-saturated with O_2) with 0.1 mM sodium azide, 25 °C, 0.1 ml min^{-1}, seventh harmonic shown. Cyclic voltammetry: 0.70 → 0.20 → 0.70 V vs. Ag|AgCl|3M NaCl, 10 mV s^{-1}.

Section S12 Effect of changing CV scan parameters

Changing to potential range over which the cyclic voltammetry significantly affected both mass and activity loss (Figure S12). Lower the value of the high-potential vertex made no difference to stability, while raising the potential of the low-potential vertex above ca. 0.6 V vs. SHE significantly improved stability and changed the pattern of inactivation to be closer to that of the chronoamperometry case.

Mass and activity are also sensitive to scan rate. Lower scan rates (e.g., Figure S13) lead to much larger losses in activity even though the mass losses are comparable to those from faster scan rates (Table S4).

There was no appreciable difference in the QCM traces when the size of the potential steps for the CVs was varied between 0.1 mV and 10 mV.

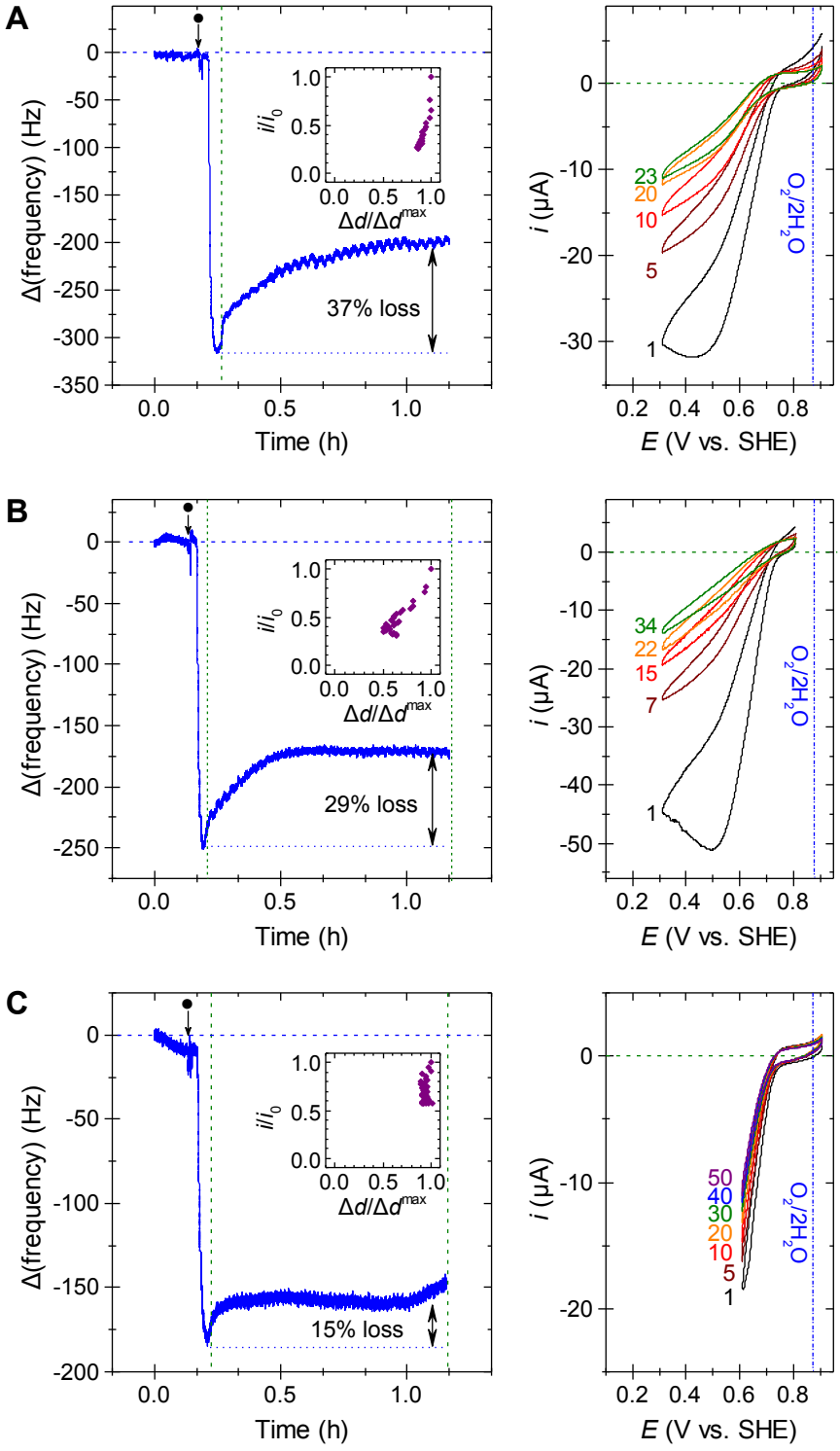

Figure S12. Frequency and electrochemical response to *Mv*BOx adsorbed on a gold-coated QCM sensor modified with 3-mercaptopropionic acid. Panel **A**: 0.70 to 0.10 V vs. Ag|AgCl|3M NaCl (full range); Panel **B**: 0.60 to 0.10 V vs. reference (keeping below potential for four-electron O_2 reduction); Panel **C**: 0.70 to 0.40 V vs. reference (keeping above potential where some reduction occurs in the absence of protein, cf. **Figure S9**). Green dashed lines indicate the period over which cyclic voltammetry scans were run. Circle (●) indicates when 25 µl 24 mg ml^{-1} *Mv*BOx was injected. The insets show the relationship between dissipation and electrocatalytic current. Conditions: 0.1 M sodium phosphate pH 6.0 (pre-saturated with O_2), 25 °C, 0.1 ml min^{-1}, seventh harmonic shown. Scan rate: 10 mV s^{-1}.

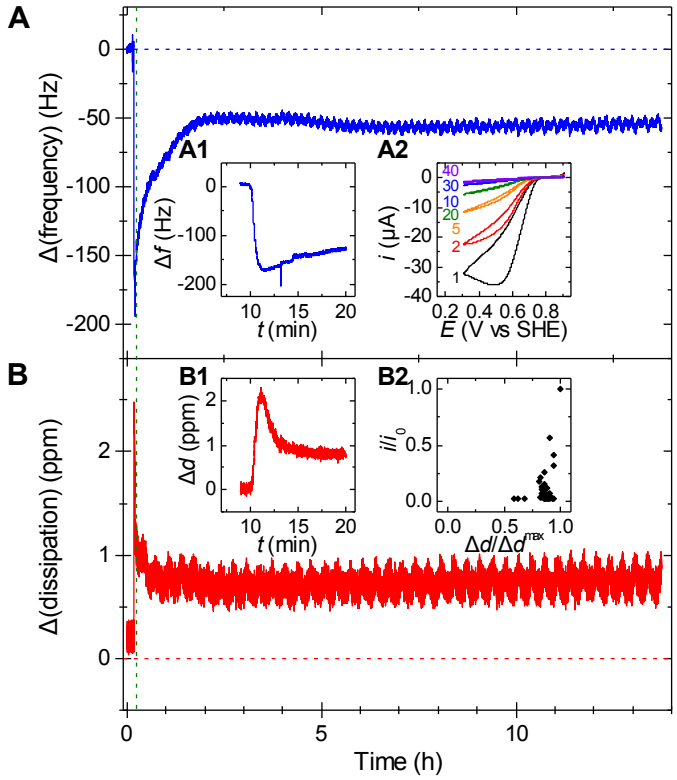

Figure S13. Frequency, dissipation and current responses to *Mv*BOx adsorbed on a gold-coated QCM sensor modified with 3-mercaptopropionic acid when the applied potential is scanned 10× more slowly than the case shown in Figure 2. Panel **A** shows the frequency change. The insets **A1** and **A2** show, respectively, a zoom of frequency during adsorption and cyclic voltammetry scans 1, 5, 10, 20, 30 and 40 of 46 scans. Panel **B** shows the dissipation response. Inset **B1** shows a zoom of the dissipation trace during adsorption. Inset **B2** shows the relation between current and dissipation during the experiment. The green dashed line indicates when cyclic voltammetry was started. Conditions: 0.1 M sodium phosphate pH 6.0 (pre-saturated with O_2), 25 °C, 0.1 ml min^{-1}, seventh harmonic shown. Cyclic voltammetry: 0.70 → 0.10 → 0.70 V vs. Ag|AgCl|3M NaCl, 1 mV s^{-1}.

Table S4. Effect of scan rate on adlayers of *Mv*BOx. Fractional losses are based on readings taken immediately cyclic voltammetry began and 20 minutes after.

scan rate (mV s^{-1})	no. scans	current loss	mass loss
0.1	100	66%	30%
0.01	10	57%	24%
0.001	1	31%	27%

Section S13 Effects of variations in oxygen saturation

The effect of swapping between oxygen and argon flow during constant potential experiments is illustrated in Figure S14. The trace shows a typical pattern of a peak in the dissipation from the formation of a loosely bound layer that washes away quickly, followed by a steady frequency response and an exponential decrease in catalytic current. Changing the buffer purge gas to argon causes the current magnitude to decrease with a first-order time constant of about 780 s; switching back to oxygen causes the current magnitude to increase with a first-order time constant of about 450 s. As indicated by the dotted line in panel **C** (a first-order exponential extrapolation of the current measured before the argon flush), the current magnitude after reoxygenation is slightly higher than would be expected in the absence of an argon purge.

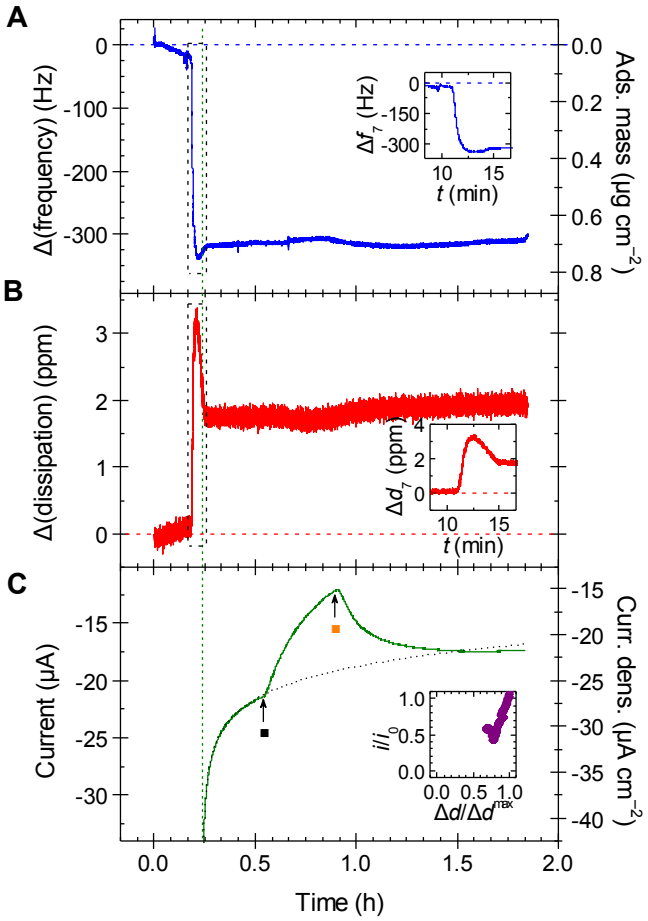

Figure S14. Frequency, dissipation and current response with time for *Mv*BOx adsorbed onto a gold-coated QCM sensor modified with 3-mercaptopropionic acid. The green dashed line shows when a potential of 0 V vs. Ag|AgCl|3M NaCl was applied. Inset in **A** and **B** shows zoomed trace of enzyme adsorption. Square (■) indicates the switch to argon gas saturated buffer solution and (■) indicates the switch back to oxygen-saturated solution. Conditions: 0.1 M sodium phosphate pH 6.0 (pre-saturated with O_2), 0.1 M sodium phosphate pH 6.0 (pre-saturated with O_2), 25 °C, 0.1 ml min^{-1}, seventh harmonic shown. Current density based on projected electrode area of 0.80 cm^2.

A 'mixed mode' measurement, in which both constant and cycled potentials were used, is shown in Figure S16. After protein adsorption, the applied potential was held constant, then argon-saturated buffer was flowed through the cell. While the oxygen was being displaced, the measurements swapped to cyclic voltammetry. Toward the end of the potential cycling, the oxygen-saturated buffer was reintroduced; some activity remained. After 25 cycles, the potential was again held constant. Both the current and frequency response at this stage were very stable.

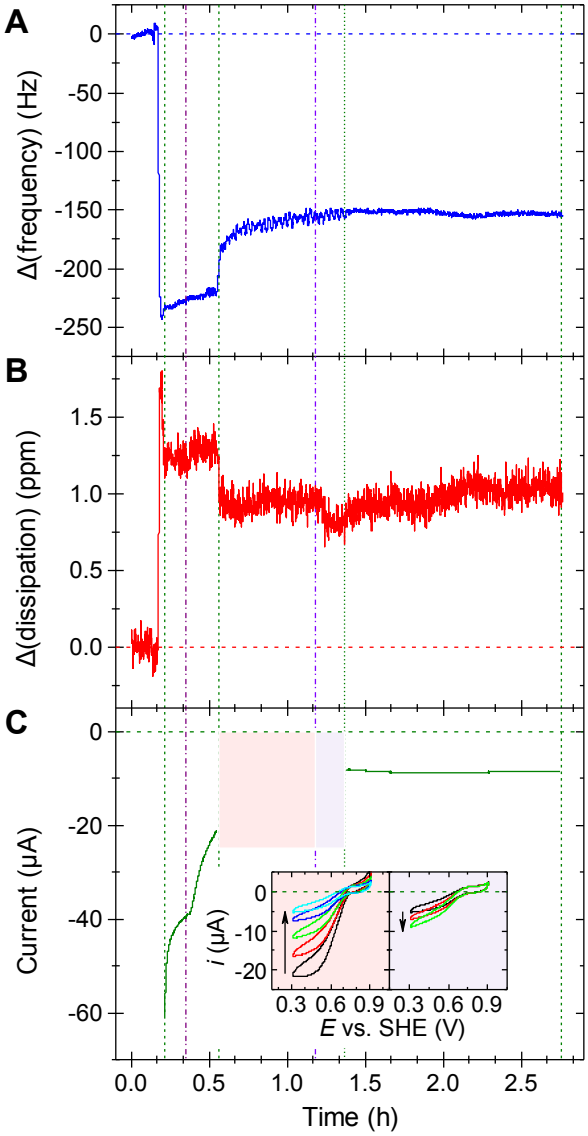

Figure S15. The effect of oxygen on the (**A**) frequency, (**B**) dissipation and (**C**) current response with time for *Mv*BOx adsorbed onto a gold-coated QCM sensor modified with 3-mercaptopropionic acid. The vertical green dashed lines represent the start and end of chronoamperometry measurements (0.1 V vs. Ag|AgCl|3M NaCl). The vertical green dotted lines represent the start and end of cyclic voltammetry (0.70 → 0.10 → 0.70 V vs. reference). The vertical purple dash-dot lines indicate when the solution flowing through the cell was changed to argon saturated buffer. The insets in Panel **C** show the decay in electrocatalytic current as O_2-satured buffer is displaced by argon-saturated solution (left inset; scans 1, 3, 6 and 19 shown) and the partial recovery of current after the argon-saturated buffer is replaced by O_2-saturated solution (right inset, scans 19, 21 and 24 shown). Conditions: 0.1 M sodium phosphate pH 6.0 (pre-saturated with O_2), 25 °C, 0.1 ml min^{-1}, seventh harmonic shown.

Section S14 Measurements on a second multicopper oxidase

We also used a second commercially available multicopper oxidase, laccase from *Trametes versicolor* (*Tv*L). The protein was adsorbed to a gold-coated quartz crystal modified with 3-mercapto-1-propanol, with the adsorption and subsequent cyclic voltammetry performed as for Figure 2 from the main text. Figure S16 shows 50 potential cycles and E-QCM-D responses that parallel those observed for *Mv*BOx.

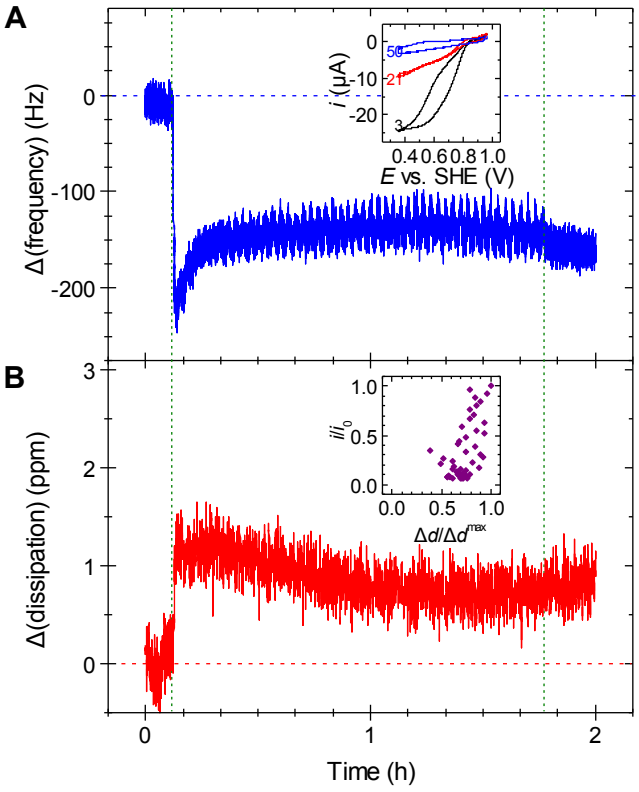

Figure S16. Frequency (Panel **A**) and dissipation (Panel **B**) response to *Tv*L adsorbed on a gold-coated QCM sensor modified with 3-mercapto-1-propanol. The green dashed line indicates when cyclic voltammetry was started and ended. Inset: Cyclic voltammetry of *Tv*L on 3-mercapto-1-propanol. Inset in **A** shows scans 3, 21 and 50; inset in **B** shows the relationship between current and dissipation at each low-potential vertex. Conditions: 25 °C, 0.1 M sodium citrate pH 4.0 (pre-saturated with O_2), 0.1 ml min^{-1}, seventh harmonic. Potential range: 0.75 → 0.15 → 0.75 V vs. Ag|AgCl|3M NaCl, 10 mV s^{-1}.

To compare the effect of covalent attachment to enzymes other than *Mv*BOx (Figure 3, main text) we attached *Tv*L to a DTSSP-modified gold crystal. The covalent attachment occurs through a single reactive lysine residue, Lys174,[17] which is ~32 Å away from the T1 centre, too far for efficient electron transfer from the electrode.[13] The loss of activity is further highlighted in the near absence of a catalytic wave upon potential cycling (panel **A** inset). In contrast to the observations for *Mv*BOx in Figure 3, the frequency magnitude increased when the potential was cycled, though the current vs. dissipation trace (panel **B** inset) was similar.

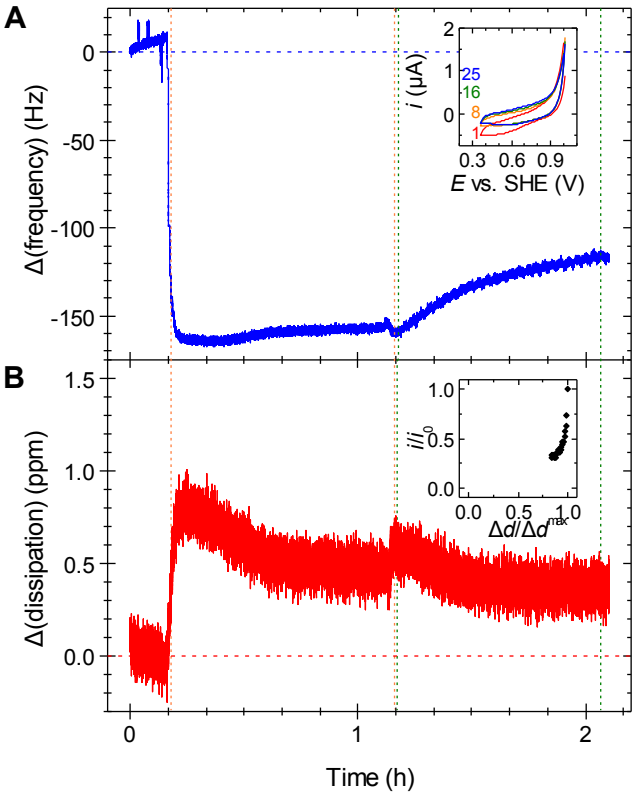

Figure S17. Frequency and dissipation response with time for *Tv*L covalently bound via an amide linkage to a DTSSP-modified QCM sensor. The orange dashed lines represent the time left for enzyme to react with surface layer (reaction adapted from the ref. 18) during which time the peristaltic pump was turned off. The green dashed line shows when potential cycling began with the inset in **A** showing the cyclic voltammograms from scans 1, 8, 16 and 25 of 25 scans. **B** shows the dissipation during enzyme adsorption and the subsequent change on potential cycling. Conditions: O_2-saturated 0.1 M sodium phosphate buffer pH 6.0 at 25 °C flowing at 0.1 ml min^{-1} with continuous O_2 bubbling, seventh harmonic shown. Cyclic voltammetry (CV): 0.80 → 0.15 → 0.80 V vs. Ag|AgCl|3M NaCl, 10 mV s^{-1}.

Section S15 Additional Δd_7 vs. Δf_7 traces

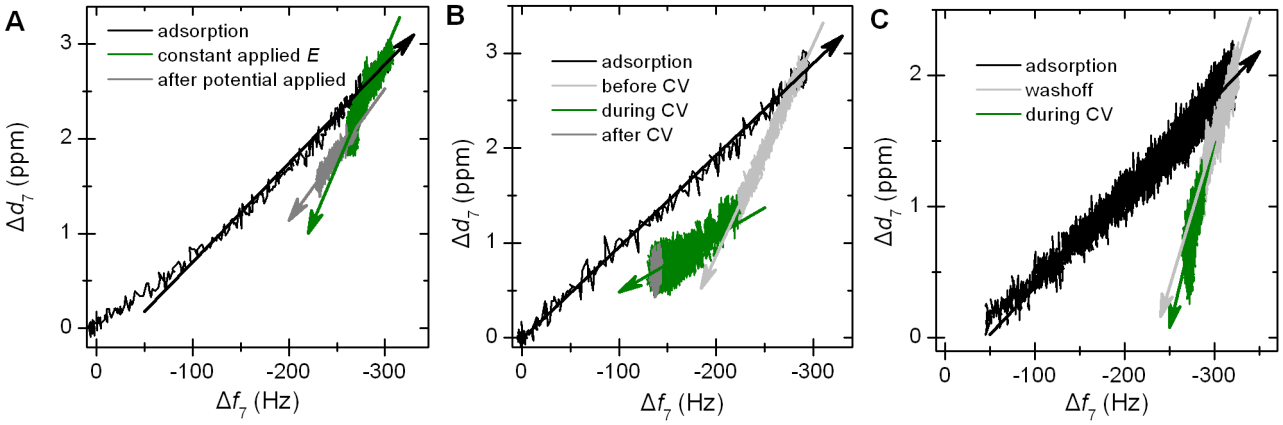

Figure S18. Plots showing correlation between energy dissipation and frequency change for the data plotted in **A** Figure 1, **B** Figure 2 and **C** Figure 3 in the main text.

Section S16 References

1. J. A. Cracknell, T. P. McNamara, E. D. Lowe and C. F. Blanford, *Dalton Trans.*, 2011, **40**, 6668-6675.
2. Q-Sense, Q-Sense E1 Module, http://www.q-sense.com/file/q-sense-e1-folder.pdf.
3. G. Sauerbrey, *Z. Phys.*, 1959, **155**, 206-222.
4. Z. Cao, Z. L. Xiao, N. Gu, S. Shimada, T. Fukuda and H. Matsuda, *Solid State Phenom.*, 2007, **121–123**, 385–388.
5. Z. Cao, L. Zhang, C.-Y. Guo, F.-C. Gong, S. Long, S.-Z. Tan, C.-B. Xia, F. Xu and L.-X. Sun, *Mater. Sci. Eng. C*, 2009, **29**, 1051-1056.
6. C. A. Widrig, C. Chung and M. D. Porter, *Journal of Electroanalytical Chemistry and Interfacial Electrochemistry*, 1991, **310**, 335–359.
7. Invitrogen, Amine-Reactive Probe Labeling Protocol | Life Technologies, http://www.invitrogen.com/site/us/en/home/References/protocols/cell-and-tissue-analysis/Labeling-Chemistry-Protocols/Amine-Reactive-Probe-Labeling-Protocol.html.
8. P. Roepstorff and J. Fohlman, *Biol. Mass Spectrom.*, 1984, **11**, 601-601.
9. R. S. Johnson, S. A. Martin, K. Biemann, J. T. Stults and J. T. Watson, *Anal. Chem.*, 1987, **59**, 2621-2625.
10. R. S. Johnson, S. A. Martin and K. Biemann, *Int. J. Mass Spectrom. Ion Processes*, 1988, **86**, 137-154.
11. V. H. Wysocki, K. A. Resing, Q. Zhang and G. Cheng, *Methods*, 2005, **35**, 211-222.
12. FindSurfaceResidues, http://www.pymolwiki.org/index.php/FindSurfaceResidues.
13. C. C. Page, C. C. Moser, X. X. Chen and P. L. Dutton, *Nature*, 1999, **402**, 47-52.
14. E. I. Solomon, U. M. Sundaram and T. E. Machonkin, *Chem. Rev.*, 1996, **96**, 2563-2605.
15. S. Trasatti and O. A. Petrii, *J. Electroanal. Chem.*, 1992, **327**, 353-376.
16. Y. Kamitaka, S. Tsujimura, T. Ikeda and K. Kano, *Electrochemistry*, 2006, **74**, 642-644.
17. J. Sobek, M.Chem. thesis, University of Oxford, 2005.
18. C. M. Moore, N. L. Akers, A. D. Hill, Z. C. Johnson and S. D. Minteer, *Biomacromolecules*, 2004, **5**, 1241-1247.